JOURNAL OF MATERIALS SCIENCE 27 (1992) 2005–2011

Effect of temperature on the strength and conductivity of a deformation processed Cu–20%Fe composite

W. A. SPITZIG, L. S. CHUMBLEY, J. D. VERHOEVEN
Ames Laboratory–USDOE, Iowa State University, Ames, IA 50011, USA

Y. S. GO
329 Bokyong-ri Ilro-yeup Muan-kun Chunnam, South Korea

H. L. DOWNING
Department of Physics, Drake University, Des Moines, IA 50311, USA

The high temperature (22–600 °C) properties were evaluated for a Cu–20%Fe composite deformation processed from a powder metallurgy compact. The ultimate tensile strengths decreased with increasing temperature but were appreciably better than those of similarly processed Cu at temperatures up to 450 °C. At 600 °C, the strength of Cu–20%Fe was only slightly better than that of Cu as a result of the pronounced coarsening of the Fe filaments. However, at temperatures of 300 and 450 °C, the strength of Cu–20%Fe is about seven and six times greater, respectively, than that of Cu, as compared to about a two fold advantage at room temperature. Therefore, Cu–20%Fe composites made by deformation processing of powder metallurgy compacts have mechanical properties much superior to those of similarly processed Cu at room temperature and at temperatures up to 450 °C. The pronounced decrease in electrical conductivity of deformation processed Cu–20%Fe as compared to Cu is attributed to the appreciable dissolution of Fe into the Cu matrix which occurred during the fabrication of the starting compacts where temperatures up to 675 °C were used. While the powder metallurgy compacts used for the starting material for deformation processing in this study did not lead to a high conductivity composite, the powder metallurgy approach should still be a viable one if processing temperatures can be reduced further to prevent the dissolution of Fe into the Cu matrix.

1. Introduction

Deformation processed metal–metal composites, especially face-centred cubic–body-centered cubic (fcc–bcc) type composites, encompass an intriguing class of materials. The fcc–bcc deformation processed metal–metal composites that have been studied include Cu–Cr [1, 2], Cu–Fe [3–6], Cu–Nb [2, 7, 8], Cu–Ta [8] and Cu–V [6]. In these types of materials, the composite is formed during the deformation processing of the ductile two phase mixture where the two phases co-deform, causing the minor phase (bcc phase) to elongate and become ribbon-like in morphology within the matrix phase (fcc phase). The greater strengthening that occurs in fcc–bcc, as compared to fcc–fcc composites, is believed to be a result of the development of the ribbon-like cross section of the bcc filaments during deformation processing. This ribbon-like filament morphology is a consequence of the {1 1 0} fibre texture that develops during cold working of bcc metals [9].

Deformation processed Cu matrix–bcc filament composites not only have very high strengths but also very good electrical and thermal conductivities and this combination of properties may be their outstanding feature. Potential applications for these composites are expected to require both their high temperature and room temperature properties. Previous work on Cu–Nb [6, 10, 11] and Cu–Ta [8] composites showed that although the strength decreased with increasing temperatures up to 600 °C, these composites retained a significant portion of their room temperature strength at the elevated temperatures. Because the Cu–Fe composite system is of special interest in light of the cheapness of Fe, as compared to the other bcc metals, further study of this system seemed warranted. While the room temperature properties of deformation processed Cu–Fe composites have been investigated earlier [2–5], only limited results are available on the high temperature mechanical properties of this composite system [3]. In the earlier study [3], the effect of annealing temperature on the mechanical properties of a Cu–15vol.%Fe composite was studied, whereas, in this study the tensile properties of a Cu–20vol.%Fe composite at temperatures up to 600 °C were evaluated. In addition, microstructural characterization of the effects of temperatures up to 600 °C on the stability of the filaments were evaluated by scanning electron

0022–2461 © *1992 Chapman & Hall*

microscopic (SEM) and transition electron microscopic (TEM) analyses for correlation with the changes in tensile properties. The mechanical properties and microstructures of the Cu–20%Fe composite at room temperature have been reported [5].

2. Materials and procedures

The Cu powder used in the compact was gas atomized in the presence of a small partial pressure of oxygen, then reduced. The mean size was about 14 μm as determined by X-ray turbidimetry. The Fe powder used in the compact was 53 μm and was water atomized. The Cu and Fe powders were mixed to give a Cu–20vol.%Fe compact which was processed by placing the powder mixture in a can and heating at 675 °C for 4 h under flowing hydrogen. The powder compact was removed from the can, bagged and isostatically pressed at 380 MPa, then rebagged and repressed at 620 MPa to give a relative density of 0.95. After pressing, the compact was about 7.5 cm in diameter and 20 cm long. Fig. 1a shows the structure of the compact after pressing. The compact was then placed in a Cu can and welded shut, heated at 500 °C for 2.5 h and extruded to a 2 cm diameter rod. After extrusion the relative density was 0.99 and this was taken to be the starting point for evaluating the effect of deformation processing on strengthening.

The extruded bar was then reduced to a diameter of 0.79 mm by cold swaging at 22 °C, reversing the direction of swaging after each pass. The Cu jacket was removed at a diameter of 1.27 mm. The wire was further reduced by drawing through successively smaller dies at 22 °C to a final diameter of 0.35 mm. The smallest wire diameter corresponds to a reduction of area of 99.97% or $\eta = 8.1$, where $\eta = \ln(A_0/A)$ and A_0 and A are the as extruded and final cross-sectional areas, respectively. This draw ratio was chosen so that the high temperature mechanical properties of Cu–20%Fe could be directly compared with those of Cu–20%Nb [11]. Fig. 1b and c show longitudinal and transverse sections, respectively, of the compact after deformation processing to $\eta = 3.3$. The longitudinal section (Fig. 1b) shows that the Fe powders adopt a filamentary morphology during deformation processing. The transverse section (Fig. 1c) reveals the convoluted ribbon-like morphology of the filaments, which is typical for bcc filaments in a fcc matrix [2, 3, 5–8].

Tensile tests were done at temperatures up to 600 °C in a stainless steel retort using a flowing argon atmosphere to prevent oxidation of the specimens during a test. All tensile tests were done at a nominal strain rate of $3.3 \times 10^{-4}\,s^{-1}$. The tensile specimens were annealed for 24 h in a vacuum furnace at their respective test temperatures prior to tensile testing to stabilize the microstructure.

Both SEM and TEM analyses were carried out of microstructural changes after annealing at various temperatures. Sample preparation procedures for the TEM specimens were similar to those reported previously for Cu–20%Nb [12]. In addition, filaments were extracted from some deformation processed Cu–20%Fe wires after annealing at various temperatures for examination of filament coarsening by dissolving the Cu matrix in an acidic solution (80 ml H_2O, 10 g $K_2Cr_2O_7$ and 5 ml H_2SO_4). These extracted filaments were examined in the SEM.

Electrical resistivity measurements were made on the deformation processed Cu–20%Fe up to a temperature of 600 °C to evaluate the electrical conductivity and to detect microstructural changes. A standard four-probe dc technique was used, as has been previously described in detail [13], and samples were heated at a rate of 1 °C min^{-1} followed by furnace cooling to room temperature.

3. Experimental results

The tensile true stress–true strain curves for specimens of the Cu–20%Fe composite drawn to $\eta = 8.1$ are shown in Fig. 2 after annealing for 24 h and testing at temperatures 150, 300, 450 and 600 °C. The curve for the as-drawn specimen tested at room temperature is also shown for comparison. The true strain to fracture

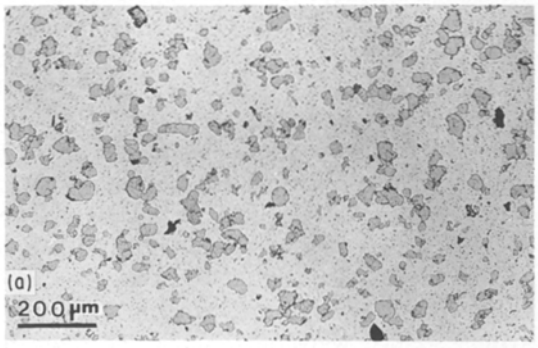

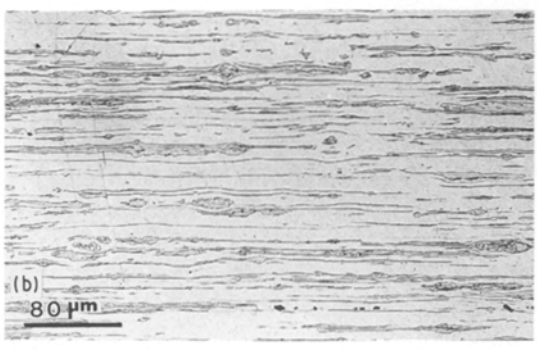

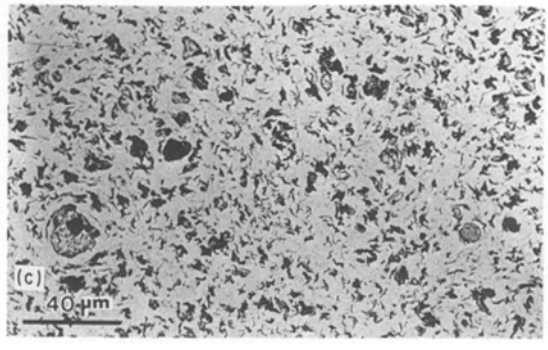

Figure 1 Optical micrographs of Cu–20%Fe; (a) original compact; (b) and (c) longitudinal and transverse sections, respectively, after drawing to $\eta = 3.3$.

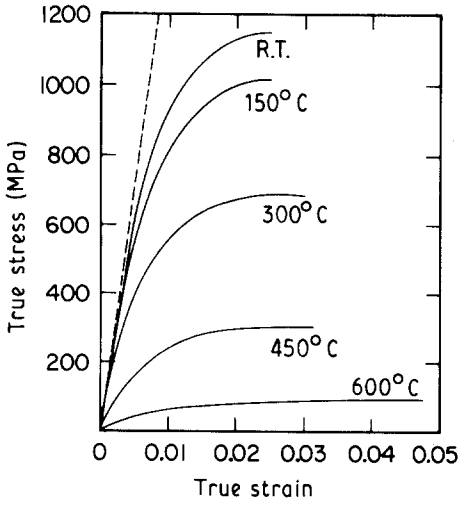

Figure 2 True stress–true strain curves of Cu–20%Fe drawn to $\eta = 8.1$ at temperatures between 22 and 600 °C.

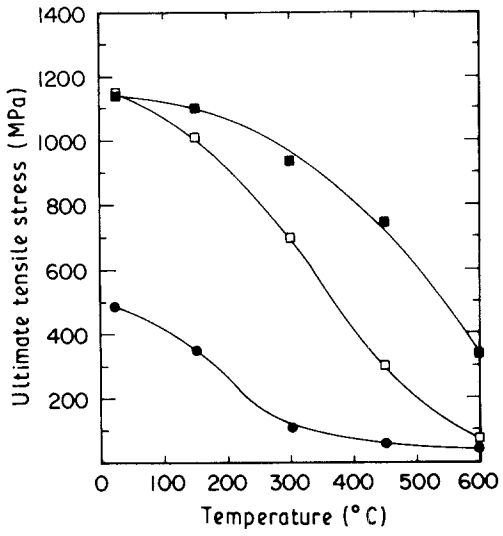

Figure 3 Effect of annealing (24 h) and testing at temperatures between 22 and 600 °C on the ultimate tensile stress of Cu, Cu–20%Fe and Cu–20%Nb drawn to $\eta = 8.1$. (□) Cu–20%Fe (C, < 53μmFe); (■) Cu–20%Nb (cast); (●) Cu.

increases with increasing temperature, particularly at 600 °C. The dashed line in Fig. 2 is the elastic modulus which has a slope of 145 GPa, which is the rule of mixtures elastic modulus of the Cu–20%Fe composite. The pronounced decrease in the ultimate tensile strength of deformation processed Cu–20%Fe with increasing temperature is clearly evident in Fig. 3. Also included in Fig. 3 are previous data for similarly deformation processed Cu and Cu–20%Nb [11]. The Cu–20%Nb was made by an arc-casting process rather than a powder metallurgy process but strengthening has been shown to be similar with subsequent deformation processing for both initial compact formation processes [14]. While the strengths of Cu–20%Fe and Cu–20%Nb were similar at room temperature, the strength of Cu–20%Fe was always appreciably lower than that of Cu–20%Nb as the temperature increased. At 600 °C the strength of Cu–20%Fe is about the same as that of Cu.

SEM micrographs of longitudinal sections of the Cu–20%Fe wires annealed for 24 h at 300, 450 and 600 °C are shown in Fig. 4. Filament coarsening was apparent at 300 °C (Fig. 4a) and was pronounced at 450 and 600 °C (Fig. 4b and c). The spacings and thicknesses of the filaments are increased because of filament coarsening which becomes more pronounced as the temperature is increased. However, as will be shown in the next section, the morphology of the filaments also changes as a result of heating at the higher temperatures.

4. Discussion of results

The strength of a deformation processed Cu–20%Fe composite annealed and tested at temperatures up to 600 °C was shown to rapidly decrease with temperature, especially above 300 °C, although it was always stronger than Cu. The decreasing strength with temperature in similarly deformation processed Cu–20%Nb and Cu–20%Ta was shown to be primarily a consequence of filament coarsening [11, 13]. The better high temperature strength properties in Cu–20%Ta as compared to Cu–20%Nb were attributed to the higher melting temperature of Ta as compared to Nb, which is expected to decrease the tendency for surface diffusion and coarsening in the former composites at a given temperature [11].

Fig. 5 shows Fe filaments that were extracted from the deformation processed wires that were annealed for 24 h at 300, 450 and 600 °C. Filament coarsening was not apparent in filaments extracted from wires heated to 150 °C for 24 h. After heating to 300 °C, some of the filaments show signs of coarsening at the surfaces (Fig. 5a). After annealing at 450 and 600 °C for 24 h (Fig. 5b and c), coarsening of the filaments is readily apparent, especially at the higher temperature. Nonuniformity of the filament surface becomes apparent at these higher temperatures and the filaments are starting to break up and show signs of pinching off and spheroidization. The ribbon-like filaments are being converted into rods, thereby changing the convoluted lamellar phase into a row of cylindrical fibres, each of which can be converted into a row of globular particles. This appears to be typical of the progression of coarsening observed in Cu–Fe [15] and in lamellar structures in general [16].

Fig. 6 shows the measured filament spacings, λ, and thicknesses, τ, using standard intercept procedures [17] on micrographs similar to those in Fig. 4 from specimens annealed for 24 h at the different temperatures up to 600 °C. The increase in spacing and thickness with increasing temperature is apparent. At 22 °C the strength of the Cu–20%Fe composite was described by the relation

$$\sigma = \sigma_0 + k\lambda^{-1/2} \quad (1)$$

where σ is the ultimate tensile stress, $k = 1230$ MPa $\mu m^{-1/2}$ and $\sigma_0 = 0$ [5]. The increase in filament spacing can account for the strength decrease up to 300 °C but, at 450 and 600 °C, the decrease in ultimate tensile stress is much more pronounced than that which can be attributed to spacing alone. For example, at 450 and 600 °C the stress predicted from Equation 1 is 652 and 528 MPa, respectively, as compared to the observed values of 300 and 70 MPa (Fig. 3), respectively.

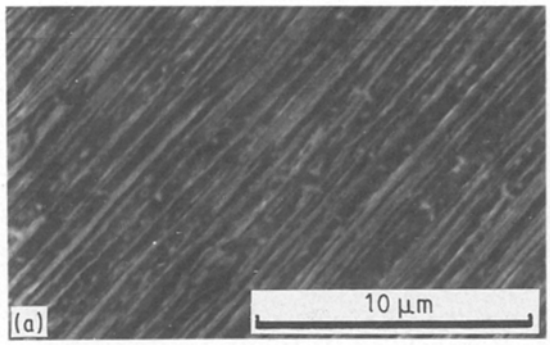

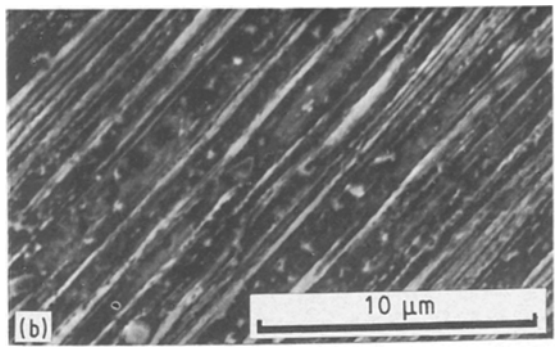

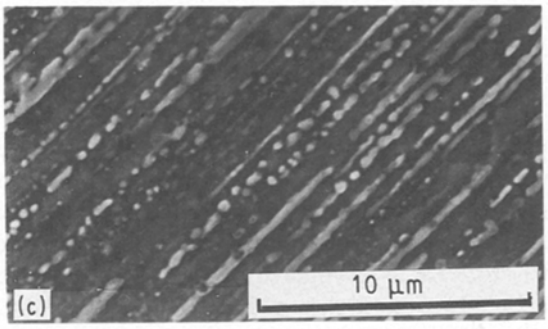

Figure 4 Longitudinal sections of Cu–20%Fe drawn to $\eta = 8.1$ which were annealed for 24 h at (a) 300 °C, (b) 450 °C and (c) 600 °C. Cu slightly etched away to reveal Fe filaments.

This enhanced decrease in stress at these temperatures is most likely caused by the change in filament morphology in addition to the increase in filament spacing. The convoluted ribbon-like filament morphology developed during axisymmetric deformation processing imparts much higher strength at a given filament spacing than layers of the filamentary phase [18] or the aligned planar morphology that develops as a result of deformation processing by rolling [19].

Figs 7–9 show TEM micrographs of the deformation processed Cu–20%Fe composite in the as-drawn condition (Fig. 7) and after annealing for 24 h at 300 and 600 °C (Figs 8 and 9, respectively). In the as-drawn condition, the Fe filaments have a ribbon-like morphology, whereas after annealing at 300 and 600 °C for 24 h they take on a circular cross-sectional appearance in accord with their breaking up into cylinders and subsequently a row of connected globular particles. The cross-sectional size increases as the annealing temperature increases and coarsening becomes more advanced.

To gain further insight into filament coarsening in the deformation processed Cu–20%Fe composites, electrical resistivity measurements were made over the temperature range 22 to 600 °C. Electrical resistivity measurements have been shown to be very sensitive to filament coarsening in deformation processed Cu–Nb composites [13]. Fig. 10 presents resistivity versus temperature data on Cu–20%Fe, Cu–20%Nb and pure Cu wires all deformed to an η value of 8.1. The resistivity was monitored continuously as the samples were heated at a rate of 1 °C min^{-1} up to some temperature, T_{max}, held at T_{max} for 2 h and then furnace cooled to room temperature. The value of T_{max} was 600 °C for the Cu–20%Fe wire and 810 °C for the Cu–20%Nb and the pure Cu wires. Previous analyses of deformation processed Cu–Nb alloys [13, 20] have shown that there are four major contributions to the total resistivity: phonon scattering, ρ_{ph}; impurity scattering, ρ_{imp}; dislocation scattering, ρ_{dis}; and interface scattering, ρ_{int}. The upper branch of each of the curves

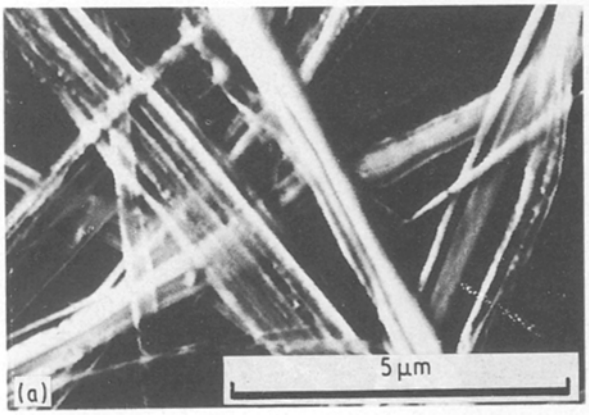

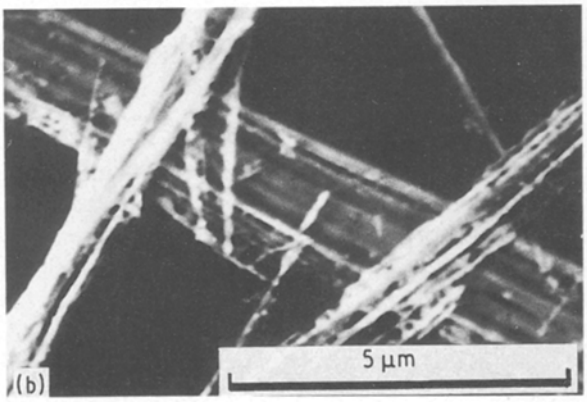

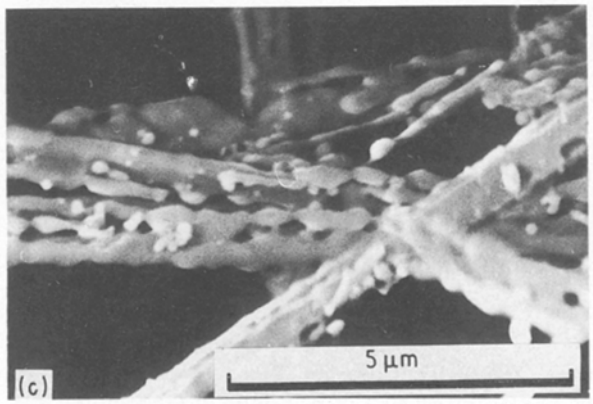

Figure 5 SEM micrographs of Fe filaments extracted from Cu–20%Fe drawn to $\eta = 8.1$ and annealed for 24 h at (a) 300 °C, (b) 450 °C and (c) 600 °C.

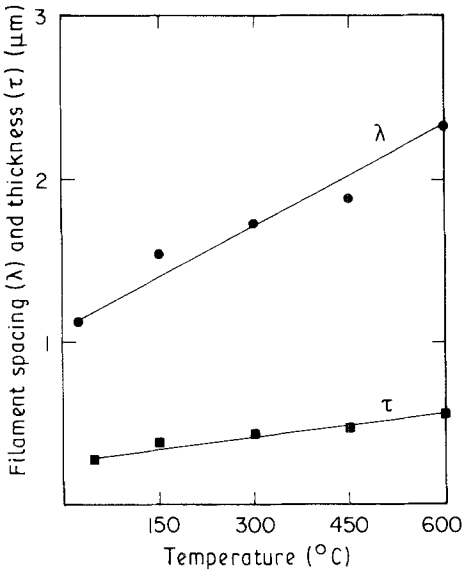

Figure 6 Spacings and thicknesses of Fe filaments in Cu–20%Fe drawn to $\eta = 8.1$ and annealed for 24 h at temperatures between 150 and 600 °C.

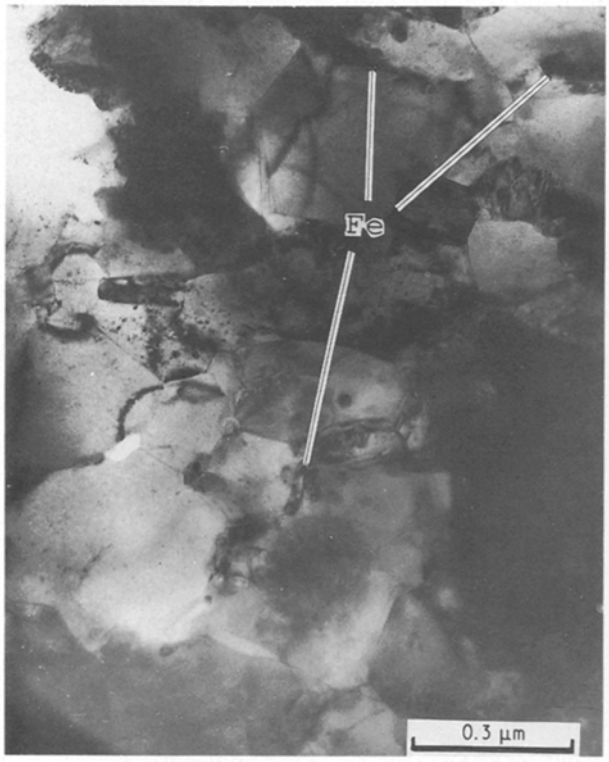

Figure 7 TEM micrograph of transverse section of Cu–20%Fe drawn to $\eta = 8.1$ in the as-drawn condition.

Figure 8 TEM micrograph of transverse section of Cu–20%Fe drawn to $\eta = 8.1$ and annealed for 24 h at 300 °C.

Figure 9 TEM micrograph of transverse section of Cu–20%Fe drawn to $\eta = 8.1$ and annealed for 24 h at 600 °C

in Fig. 10 gives the resistivity on heat-up, and it is higher than the lower branch obtained on cool-down after the 2 h hold because structural changes during heating reduce all of the scattering mechanisms except ρ_{ph}. Pure Cu is used as a standard, where the contributions of ρ_{int} and ρ_{imp} are taken as zero. The previous analysis [13] has demonstrated that for pure Cu the value of ρ_{dis} is only around 0.1 μΩ cm. Because TEM analyses [13] demonstrated that the dislocation densities in Cu–Nb alloys were essentially the same as in pure Cu deformed to the same η value, it was assumed that ρ_{dis} for the Cu–Nb alloys was also around 0.1 μΩ-cm. The microstructures of the as-deformed Cu–Fe alloys examined in TEM were very similar to those of Cu–Nb alloys deformed to the same η values with regard to dislocation density and the shape and size of the filaments. It seems reasonable, therefore, to assume that the resistivity scattering contributions from dislocations and the Cu-filament interfaces would be similar for Cu–20%Fe and Cu–20%Nb alloys at similar deformation strains. Comparing the Cu–20%Nb

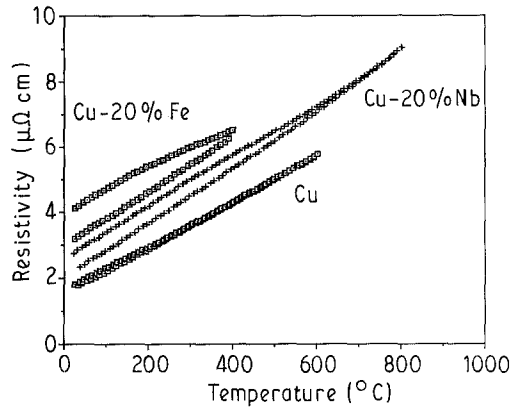

Figure 10 Comparison of the electrical resistivity as a function of temperature for Cu, Cu–20%Fe and Cu–20%Nb drawn to $\eta = 8.1$.

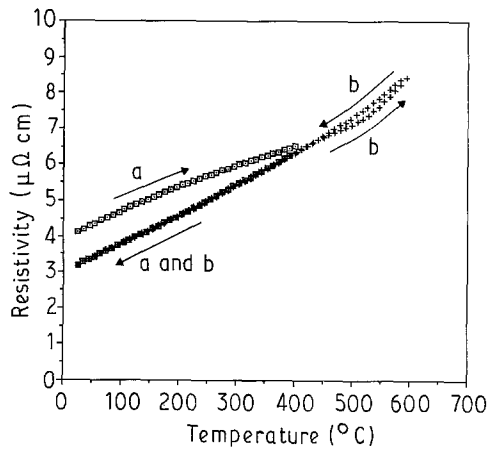

Figure 11 Electrical resistivity as a function of temperature for Cu–20%Fe drawn to $\eta = 8.1$.

upper branch to the pure Cu upper branch, the Cu–Nb curve is higher due to contributions from ρ_{int} and ρ_{imp} as well as the fact that the volume fraction Cu has been reduced by the presence of the Nb filaments. This latter effect has been accounted for by assuming a parallel circuit for the Cu matrix and the filaments [13] and it has been shown that the contribution of ρ_{imp} is 0.18 μΩ cm. The contribution of ρ_{int} is 0.30 μΩ cm at $\eta = 8.1$ before heating to T_{max}, and 0.09 μΩ cm after heating to T_{max}. The reduction in interface scattering on heating is due to the coarsening of the Nb filaments.

In comparing the Cu–20%Fe and Cu–20%Nb curves of Fig. 10, it is seen that the former curve lies considerably above the latter curve even though both alloys contain the same volume fraction of filament phase. By the above arguments it is expected that the contributions of both ρ_{dis} and ρ_{int} of the as-drawn wire should be roughly the same for Cu–20%Fe and Cu–20%Nb. This means that the much higher total resistivity of the Cu–20%Fe wire must be due to a much higher contribution from impurity scattering, ρ_{imp}. This result is not too surprising because the Cu matrix will dissolve considerably more Fe than Nb at temperatures above around 250 to 300 °C and Fe has a very large resistivity decrement in Cu, $\Delta\rho/\Delta x = 9.2$ μΩ cm/wt % Fe [21]. The dramatic effect of Fe dissolution in the Cu matrix is demonstrated by the curve labelled b in Fig. 11, which is a plot of the resistivity versus temperature on the same wire as shown in Fig. 10 (replotted in Fig. 11 as curve a) on reheating to a T_{max} value of 600 °C. Whereas the slope of the resistivity curve for Cu–Nb is found to drop continuously as the temperature rises from 400 to 600 °C, it is seen that the slope of the curve for Cu–Fe begins to increase significantly due to dissolution of Fe into the Cu matrix.

It is possible to estimate the wt % Fe dissolved in the Cu matrix, x, from the following equations:

$$\rho_{imp} = \rho_{Cu} - \rho_{ph} - \rho_{int} - \rho_{dis} \quad (2)$$

$$x = \rho_{imp}/(\Delta\rho/\Delta x) \quad (3)$$

where ρ_{Cu} is the resistivity of the Cu matrix calculated from the measured total resistivity using a parallel circuit with a volume fraction of Fe of 0.2 and the resistivity of Fe taken as 10 μΩ cm. The room temperature resistivity of pure Cu gives ρ_{ph} as 1.67 μΩ cm and, from Fig. 10, the value of ρ_{Cu} for the as-drawn Cu–Fe wire at room temperature is calculated to be 3.57 μΩ cm. Taking $\rho_{dis} = 0.1$ μΩ cm and $\rho_{int} = 0.3$ μΩ cm, from the analysis of Cu–20%Nb alloys [13], one finds a value of $x = 0.16$ wt % Fe from Equations 2 and 3 for the as-drawn wire. It seems likely that this large amount of Fe impurity must have dissolved into the Cu powders during the 4 h hydrogen treatment at 675 °C. This conclusion is supported by examination of solubility data for Fe in Cu. Data in Hansen and Anderko [22] were plotted as log x versus $1/T$ and the following correlation was obtained, $x = 2540 \exp(-8800/T)$. The correlation predicts an equilibrium solubility of 0.24 wt % Fe in Cu at 675 °C, which is consistent with the conclusion that the 4 h, 675 °C hydrogen treatment dissolved 0.16 wt% Fe into the Cu powder particles. It is likely that the 500 °C extrusion step made only a minor contribution to the dissolution of the Fe, as the predicted equilibrium solubility at 500 °C is only 0.029 wt % Fe.

It is seen from Fig. 11 that the Cu–Fe wire has the same resistivity at room temperature after the 2 h holds at the T_{max} values of 400 or 600 °C. If it is assumed that the amount of coarsening in these treatments is the same as that which occurred in the Cu–20% Nb alloys at 810 °C (which is reasonable in view of the greater coarsening kinetics of Fe versus Nb), then ρ_{int} may be taken as 0.09 μΩ cm and the value of x calculated from Equations 2 and 3 is 0.085 wt % Fe. This value is significantly higher than the equilibrium solubility value calculated from the above equation at 400 °C, which is only 0.005 wt % Fe. This result indicates that the Fe dissolved in the Cu at the high temperatures is not precipitating out during the furnace cooling or during the 2 h hold at 400 °C, a result that is consistent with previous work on cast Cu–Fe alloys [4] which found that thermomechanical processing was necessary to enhance the low temperature precipitation process.

Even though the powder processed Cu–20%Fe of this study has equivalent strength to Cu–20%Nb [5], its higher resistivity makes it less attractive for practical applications. For example, the room temperature electrical conductivity of the Cu–20%Nb alloy of Fig. 10 is 62% IACS (International annealed copper standard), as compared to only 42% IACS for the

Cu–20%Fe alloy. It is clear that Cu–Fe composites will not be suitable replacements for Cu–Nb composites in situations where both high strength and high conductivity are required unless the conductivity of the Cu–Fe composites can be improved. This means that Cu–Fe composites must be processed at lower temperatures than used in this study (675 °C) so that the solubility of Fe in the Cu matrix is kept sufficiently low so that the conductivity of the composite is not appreciably decreased.

5. Summary and conclusions

The ultimate tensile stress of a Cu–20%Fe composite deformation processed from a powder metallurgy compact rapidly decreased with increasing temperatures up to 600 °C but its strength was significantly better than that of similarly processed Cu at all temperatures except 600 °C, where it was only slightly better. However, at temperatures of 300 and 450 °C the strength of Cu–20%Fe is about seven and six times greater, respectively, than that of Cu, as compared to about a two fold advantage at room temperature. Therefore, Cu–20%Fe composites made by deformation processing of powder metallurgy compacts have mechanical properties much superior to those of similarly processed Cu at room temperature and at temperatures up to 450 °C. However, while deformation processed Cu–20%Fe is slightly stronger than similarly processed Cu–20%Nb at room temperature [5], its high temperature properties are inferior, particularly at temperatures above 300 °C. These inferior high temperature properties are believed to be a consequence of the greater tendency for filament coarsening in Cu–Fe because of the greater mobility of Fe atoms relative to Nb atoms, which is inferred from the lower melting temperature of Fe. Therefore, Cu–Fe composites will have inferior strength properties compared to Cu–20%Nb composites at high temperatures, particularly above 300 °C.

The pronounced decrease in electrical conductivity of deformation processed Cu–20%Fe as compared to Cu or Cu–20%Nb is attributed to the appreciable dissolution of Fe in the Cu matrix which occurred as a result of the fabrication of the starting compacts. While the powder metallurgy compacts used for the starting material for deformation processing in this study did not lead to a high conductivity composite, the powder metallurgy approach should still be a viable one if processing temperatures can be reduced so as to prevent the dissolution of Fe into the Cu matrix.

Acknowledgements

The authors thank L. K. Reed for experimental assistance, H. H. Baker for metallographic work and C. L. Trybus for preparation of the initial Cu–20%Fe powder metallurgy compacts. This work was performed for the U.S. Department of Energy by Iowa State University under contract No. W–7405–Eng–82. This research was supported by the Director of Energy Research, Office of Basic Energy Sciences.

References

1. P. D. FUNKENBUSCH, T. H. COURTNEY and D. G. KUBISCH, *Scripta Metall.* **18** (1984) 1099.
2. P. D. FUNKENBUSCH and T. H. COURTNEY, *ibid.* **15** (1981) 1349.
3. J. C. MALZAHN KAMPE and T. H. COURTNEY, *ibid.* **20** (1986) 285.
4. J. D. VERHOEVEN, S. C. CHUEH and E. D. GIBSON, *J. Mater. Sci.* **24** (1989) 1748.
5. Y. S. GO and W. A. SPITZIG, *ibid.*, in press.
6. J. BEVK, W. A. SUNDER, G. DUBLON and D. C. COHEN, in "In Situ Composites IV", edited by F. D. Lemkey, H. E. Cline and M. McLean (Elsevier, New York, 1982) p. 121.
7. W. A. SPITZIG, A. R. PELTON and F. C. LAABS, *Acta Metall.* **35** (1987) 2427.
8. W. A. SPITZIG and P. D. KROTZ, *ibid.* **36** (1988) 1715.
9. W. F. HOSFORD Jr, *Trans. Met. Soc. AIME* **230** (1964) 12.
10. J. BEVK and K. R. KARASEK, in "New Developments and Applications in Composites", edited by D. Kuhlman-Wilsdorf and W. C. Harrigan Jr (TMS–AIME, Warrendale, PA, 1979) p. 101.
11. P. D. KROTZ, W. A. SPITZIG and F. C. LAABS, *Mater. Sci. Engnr.* **A110** (1989) 37.
12. L. S. CHUMBLEY, H. L. DOWNING, W. A. SPITZIG and J. D. VERHOEVEN, *ibid.* **A117** (1989) 59.
13. J. D. VERHOEVEN, H. L. DOWNING, L. S. CHUMBLEY and E. D. GIBSON, *J. Appl. Phys.* **65** (1989) 1293.
14. C. L. TRYBUS, W. A. SPITZIG, J. D. VERHOEVEN and F. A. SCHMIDT, in "Processing and Properties for Powder Metallurgy Composites", edited by P. Kumar, K. Vendula and A. Ritter (TMS, Warrendale, PA, 1988) p. 97.
15. J. C. MALZAHN KAMPE, T. H. COURTNEY and Y. LENG, *Acta Metall.* **37** (1989) 1735.
16. T. H. COURTNEY and J. C. MALZAHN KAMPE, *ibid.* **37** (1989) 1747.
17. E. E. UNDERWOOD, in "Quantitative Stereology" (Addison-Wesley, Reading, MA, 1970) Chs 3 and 4.
18. R. K. EVERETT, *Scripta Metall.* **22** (1988) 1227.
19. C. L. TRYBUS and W. A. SPITZIG, *Acta Metall.* **37** (1989) 1971.
20. K. R. KARASEK and J. BEVK, *J. Appl. Phys.* **52** (1981) 1370.
21. A. BOLTAX, *Trans. Met. Soc. AIME* **218** (1960) 812.
22. M. HANSEN and K. ANDERKO, in "Constitution of Binary Alloys", 2nd Edn (McGraw-Hill, New York, 1958) p. 580.

Received 14 February
and accepted 3 December 1990